Supramolecular recognition in crystalline nanocavities through Monte Carlo and Voronoi network algorithms

Daniel Schwalbe-Koda and Rafael Gómez-Bombarelli*

Department of Materials Science and Engineering, Massachusetts Institute of Technology, Cambridge, MA 02139

E-mail: rafagb@mit.edu

Abstract

Computational screening of templating molecules enables the discovery of new synthesis routes for zeolites. Despite decades of work in molecular modeling of organic structure-directing agents (OSDAs), the development and benchmarking of algorithms for docking molecules in nanoporous materials has received scarce attention. Here, we introduce Voronoi Organic-Inorganic Docker (VOID) a method based on Voronoi diagrams to dock molecules in crystalline materials, and release it as a Python package. Benchmarks of the implementation show it generates docked poses up to 95 times faster than the traditional Monte Carlo docking scheme. We then evaluate the algorithm by obtaining binding energies for about 120 zeolite-OSDA pairs of industrial relevance. The computed host-guest interactions explain experimental outcomes for traditional synthesis routes from the literature. The results further suggest new OSDAs to synthesize known zeolites. Finally, we exemplify the generality of VOID by docking molecules inside a metal-organic framework and on a metal surface. The proposed method and

software provide a low-cost computational approach for generating molecule-material interfaces.

Introduction

Zeolites are inorganic materials with broad industrial relevance. Their metastable, yet robust nanoporous structure provides high shape and size selectivity for applications in catalysis, separation, ion exchange and others.[1] Despite decades of sustained research in zeolite discovery, little over 250 different zeolite topologies have been experimentally identified.[2,3] Whereas some of these are found in nature as minerals, most industrially-relevant zeolites are synthetic. The traditional hydrothermal synthesis of zeolites employs organic structure-directing agents (OSDAs) as reactants to target certain frameworks.[4,5] In this case, charge mismatch and short range interactions direct the formation of topologies that act as best hosts for that particular molecule.[6–8] However, finding descriptors to explain and control the synthesis of a given zeolite is still a major challenge, which often relies on trial and error.[9,10]

Molecular modeling plays an important role in quantifying the templating ability of OSDAs towards certain frameworks. Early approaches used shape-matching methods, such as overlap of van der Waals radii, to determine whether a molecule fits in certain pores or cavities.[11] Subsequent investigations have shown that the interaction energy between the OSDA and the framework is a better predictor of the product phase, induction time and other kinetic factors.[7,12–16] These results have enabled a simulation-first strategy for targeting zeolites from *de novo* designed OSDAs, producing a flurry of new discoveries over the last years.[17–21]

From a computational standpoint, there are two major obstacles to modeling OSDA-zeolite interactions: generating low-energy poses that are representative of the microscopic phase space accessible during the zeolite synthesis; and quantifying their energy. Several levels of theory have been used to predict the latter, e.g. through different interatomic

potentials or density functional theory. However, only a few docking algorithms addressing the former have been reported so far, including Monte Carlo,[22,23] Fourier transform,[24,25] steric hindrance,[26] and grower methods.[27,28] Furthermore, despite decades of study in the field, no open-source software is available to perform such a task.

Here, we describe an approach to automating molecular docking in zeolites. In particular, this work provides the following contributions:

1. Introducing an algorithm to dock molecules in zeolites based on Voronoi networks that surpasses the traditional Monte Carlo docking in generating low-energy structures, often demanding less computational resources;

2. Validating the docking methods with atomistic simulations and the zeolite literature, demonstrating close agreement between experimental outcomes and predicted host-guest interaction energies; and

3. VOID: Voronoi Organic-Inorganic Docker, an open-source Python package implementing the docking of molecules in condensed-phase structures.* While the application discussed here is comprised mostly of OSDAs in zeolites, the package is multipurpose and can be used to generate structures for other classes of adsorbates with other substrates, including metal-organic frameworks, porous polymers, and surfaces in general.

Methods

Docking algorithms

The VOID package makes extensive use of Zeo++[29,30] to calculate Voronoi nodes, and `pymatgen`[31] to manipulate crystal structures and molecules. An overview of the Voronoi docking algorithm implemented in VOID is seen in Fig. 1. The corresponding algorithm

*Available under the MIT License at: `https://github.com/learningmatter-mit/VOID`

for the traditional Monte Carlo docking is shown in Fig. S1. We follow the traditional vocabulary from the supramolecular recognition community, with the zeolite structure named as host, OSDAs as guests, and the zeolite-molecule pair as complex.[32] Each specific conformation of the molecule inside a zeolite is called a pose, to which a score (or fitness) is assigned. The higher the score, the more favorable the binding. To interface docking and scoring, VOID contains three main parts: samplers, dockers and fitness functions. Samplers are responsible for calculating the points where to attempt docking. Dockers manipulate positions of molecules and crystals to generate poses. Finally, fitness functions evaluate a pose and associate a score to it, thus verifying if the guess leads to a strong affinity. A brief description of each of them is given below.

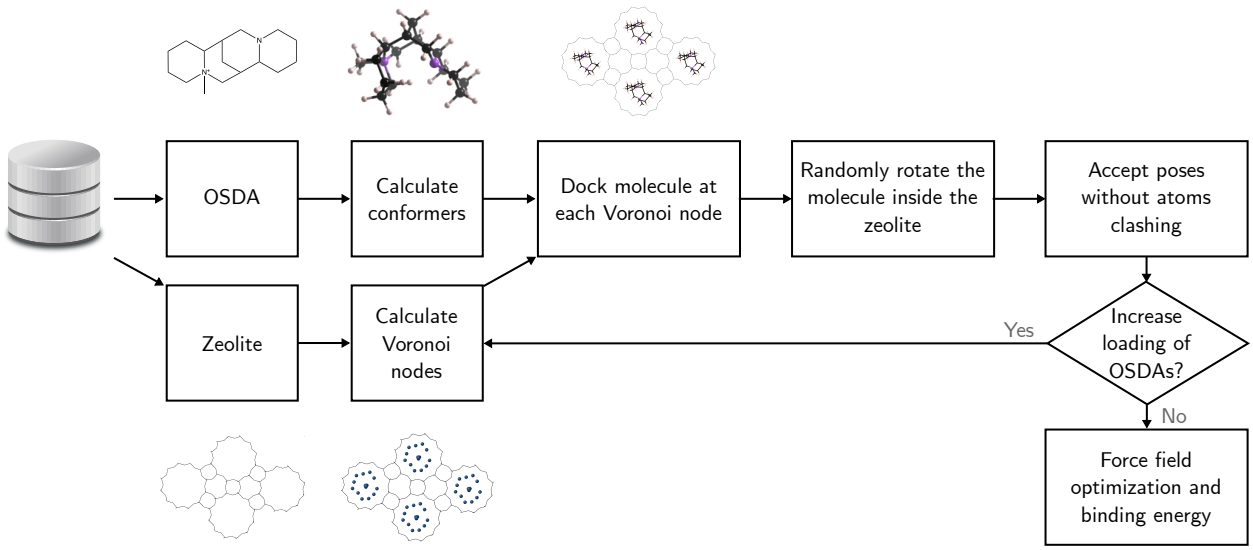

Figure 1: Flow chart of the Voronoi docking algorithm. Molecular conformers are docked at Voronoi nodes inside the framework with random orientations until no other guest can be added without violating the distance constraints.

Samplers and Voronoi nodes

Samplers analyze a loaded or semi-loaded crystal structure and return a set of points in the crystal where docking a molecule is likely to be successful. In the Voronoi docking approach, these points are the Voronoi nodes of the input structure, i.e. points in the three-dimensional space equidistant to four or more host atoms. As local and global maxima of

distances between points inside the crystal structure and the host atoms are also Voronoi nodes, they represent regions where a docked molecule would be less prone to overlap with the framework. Fig. 2 shows examples of Voronoi nodes for CHA and AFI zeolites, where nodes are located in central regions of cages and pores.

Since a multitude of Voronoi nodes exist in systems with a large number of atoms, it is computationally desirable to prune points overly close to the framework. Placing a molecule in any of these regions would be unfavorable due to their proximity to host atoms, thus generating structures with high-energy repulsive interactions. To circumvent this problem, we assign a radius for each node given by

$$d_{\text{node}} = \min_{h} \|\mathbf{r}_{\text{node}} - \mathbf{r}_h\|_2 \,, \tag{1}$$

where h is each atom in the host, $\mathbf{r}_{\text{node/h}}$ is the position of the node/host atom and $\|.\|_2$ is the Euclidean norm. The value of d_{node}, thus, is the radius of the maximum included sphere centered on that node. Then, we remove points adjacent to the structure by setting a threshold for the Voronoi node radii. Fig. S2 shows an example of Voronoi nodes calculated for different thresholds. A threshold of 3 Å was found to be effective, as higher values typically overlook regions where docking would be possible and smaller ones result in excessive clashes.

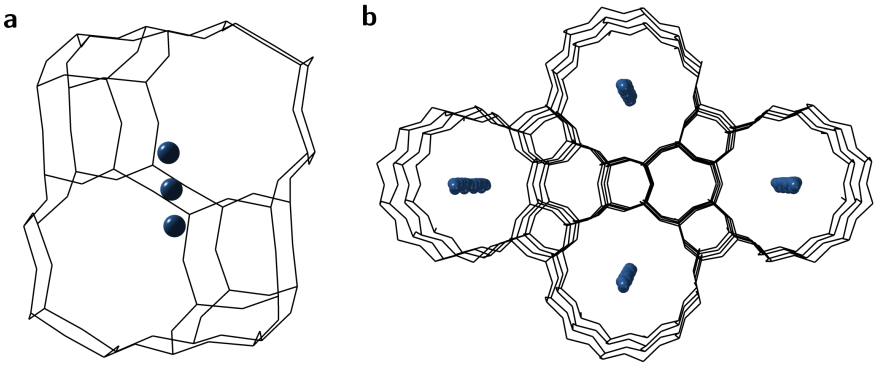

Figure 2: Perspective view of Voronoi nodes in **a**, CHA, and **b**, AFI zeolites. The nodes correspond to local maxima of distance to the atoms in the framework. The shown Voronoi nodes, depicted with blue spheres, are at least 3.5 Å away from the framework.

Since the number of Voronoi nodes can also change due to symmetry breaking and numerical imprecision in atomic coordinates, attempting to dock a molecule at all points is redundant and costly. Therefore, the number of sampled Voronoi nodes has to be limited without removing the exploration capacity of the docking scheme. We use a k-means clustering algorithm in Cartesian coordinates without periodic boundary conditions to separate the points into a constant number of regions. Then, we select the Voronoi nodes with the highest radii within each cluster as the guess points where to dock the molecule. We found that 5–10 clusters allow sufficient exploration of the void space without incurring significant overhead in computational cost.

Another possibility to reduce the number of Voronoi nodes in zeolite frameworks is to remove the oxygen atoms from the framework before generating the Voronoi diagram. In this case, only T atoms (T = Si, Al, P, etc) in the crystal are taken into account when calculating distances. A larger number of atoms typically leads to an increased number of Voronoi nodes, since the distance scalar field will contain more local maxima. Hence, removing oxygen atoms reduces the number of Voronoi nodes generated for each zeolite framework. Fig. S3 illustrates the difference of spatial distribution of nodes calculated with and without oxygen atoms.

Dockers

The Voronoi docker takes as inputs a substrate structure, a conformer for a given molecule, and the points given by the sampler. Then, it performs several trials to generate poses for the zeolite-OSDA complex. Within the Voronoi docking algorithm, the center of mass of each molecular conformation is first fixed at each Voronoi node provided by the sampler. Then, the conformer undergoes a random rotation around an axis passing through this point. These operations can be performed sequentially by the docker until all sampled points are explored. However, since rotation attempts are independent, the operations can be parallelized by using tensorial operations. The batch Voronoi docker, as implemented

in VOID, allows a large number of structures to be generated in roughly the same amount of time taken by a single, sequential attempt, although at the expense of a larger memory usage.

On the other hand, the Monte Carlo docker does not take points from a sampler as one of its inputs. Instead, it performs one of the following two actions: randomly translating the molecule inside the zeolite by sampling a vector from a multivariate Gaussian distribution with mean zero and covariance matrix equal to a multiple of the identity matrix; or randomly rotating the same molecule around its center of mass. Then, the new pose is accepted or rejected according to the Metropolis-Hastings algorithm.[33] Since this method creates a Markov Chain for each docking attempt, it is not easily parallelized. On one hand, sampling a single action for the whole batch yields correlated docking outcomes. Conversely, batching independent samples from a Markov decision process at every step offers little computational improvement over performing the actions separately. Hence, we chose not to create a batch Monte Carlo docker in VOID. The sequential Monte Carlo docker also takes an optional temperature profile as input, thus allowing simulated annealing strategies to be performed. Having to find regions where the molecule fits inside the zeolite through random translations is of the major drawbacks of this approach when compared to the Voronoi docking. Nevertheless, the Monte Carlo method can still outperform the Voronoi docking method depending on the shape of the molecule and the framework. This occurs especially when the optimal position of the molecule cannot be achieved by docking its center of mass onto Voronoi nodes.

Fitness functions

A fitness function takes a pose as input and returns a scalar corresponding to its score. Whereas total energy-based metrics can be implemented as fitness functions, they would drastically increase the wall time to complete the pose generation process. Hence, we use distance criteria to assess the soundness of the geometry as a proxy to host-guest interactions.

Several distance-based rules can be proposed to quantify this goodness of fit. One option is to take the minimum distance between the host and guest,

$$d_{\min} = \min_{g,h} \|\mathbf{r}_g - \mathbf{r}_h\|_2 \,, \tag{2}$$

where g, h refer to guest/host atoms, and define a threshold fitness function,

$$f_{\min}\left(d_{\min}\right) = \begin{cases} d_{\min} - F, & \text{if } d_{\min} \geq F, \\ -\infty, & \text{if } d_{\min} < F, \end{cases} \tag{3}$$

with F an arbitrary number. Poses with $d_{\min} < F$ are immediately rejected by this fitness function, since we want to avoid overlapping the molecule with the framework and creating an unphysical, high-energy structure. We found that $F = 1.5$ Å generally yields good poses that can be rapidly and successfully refined through physics-based simulation. The minimum distance threshold is often sufficient for generating a large number of low-energy poses through the Voronoi docking algorithm.

If desirable, we can also favor the generation of poses with given distances, particularly in Monte Carlo algorithms, by adopting a Gaussian scoring function such as

$$f_{\min,\mathrm{G}}\left(d_{\min}\right) = \exp\left(-\frac{\left(d_{\min} - F\right)^2}{2\sigma^2}\right), \tag{4}$$

where σ is a tolerance for the target distance F. This fitness function is particularly useful when a molecule has to stay a distance $d_{\min} \in [F - \sigma, F + \sigma]$ away from the framework instead of simply maximizing $d_{\min}$, as Eq. (3) would favor.

VOID contains other functions beyond the minimum distance, such as the mean distances from the guest to the host atoms. The package also allows compounding different fitness functions together for improved geometrical scoring of poses.

Simulation details

Structural optimizations were performed using the General Utility Lattice Program (GULP),[34,35] version 5.1.1, through our GULPy package.[†] The BFGS and RFO optimizers were used in sequence to accelerate the convergence of the structures. The Dreiding force field[36] was used to model interactions between the zeolite and the OSDA.

Initial zeolite structures were downloaded from the International Zeolite Association database and pre-optimized using the Sanders-Leslie-Catlow force field.[37] Conformers for OSDAs were generated using RDKit[38] with the MMFF94 force field.[39,40] After the docking, we optimized the pose at constant volume.

Binding energies (E_b) between template and zeolite were calculated according to

$$E_b = \min_{\text{pose}} \left[E_{\text{pose}} - (E_{\text{zeo}} + n E_{\text{OSDA}}) \right], \tag{5}$$

in which E_{pose} is the energy of the optimized zeolite-OSDA pose, E_{zeo} is the energy of the pure-silica, unloaded zeolite with the same geometry as the docked zeolite, E_{OSDA} is the energy of the template in gas phase, and n is the number of OSDAs docked in the pose. Since several poses with different guest loadings and orientations are created, our estimate for the complex binding energy at 0 K is the minimum energy among all the calculated poses.

Results and Discussion

A timing benchmark for the Voronoi and Monte Carlo docking algorithms implemented in VOID is shown in Fig. 3. A chabazite structure docked with a single N,N,N-trimethyladamantylammonium (TMAda+) was chosen as benchmark due to the well-known size and shape similarity between the host cavity and guest molecule. 1,000 independent docking runs were performed for each algorithm on a single Intel(R) Core(TM) i9-10940X, 3.30 GHz CPU. The minimum distance threshold from Eq. (3) was used as fitness function with $F = 1.5$ Å.

[†]Available under the MIT License at `https://github.com/learningmatter-mit/gulpy`.

Voronoi nodes were generated without oxygens in the structure, $d_{\text{node}} > 3$ Å, and separated into 10 clusters. The Monte Carlo algorithm was executed with a normalized temperature of 0.1 (in fitness function units) during the first 100 steps, and 0.0 afterwards. For the CHA-TMAda+ complex, at most two different random orientations were necessary to successfully dock the molecule into the zeolite with the Voronoi docking algorithm in 50% of the runs, and 97.5% of the docking trials finished successfully within 10 attempts, as shown in Fig. 3a. In contrast, more than 75 random translations and rotations were necessary to generate a single valid pose with the Monte Carlo algorithm in 50% of the cases.

Figure 3b displays how many seconds were necessary to successfully dock TMAda+ into CHA in each of the 1,000 independent runs. Our implementation of the Voronoi docking method is on average 12.6 times faster than its Monte Carlo counterpart. If, however, we parallelize the Voronoi docking by performing 50 attempts per Voronoi node at once using the batch docker, the improvement over the sequential Monte Carlo docking is around 95 times for the CHA-TMAda+ on a single CPU.

This speedup is particularly useful when we increase the number of OSDAs per cell or increase the size of the host system. Fig. S4 shows a zeolite docked with up to 6 molecules as generated by the Voronoi docking algorithm. To increase the loading of a system, we select one pose and use it as the new input substrate. Thus, Voronoi nodes are recalculated with atoms of the framework and docked molecules as the host atoms. As a result, new nodes will also indicate positions where an additional molecule is less likely to overlap with previously added molecules.

The algorithms can also be compared according to their final pose energy. To do that, we docked 12 popular OSDAs found in the literature (see Fig. 4) covering different sizes, shapes and flexibility, into ten well-known zeolite frameworks, namely AEL, AFI, *BEA, CHA, FER, LTA, MFI, MOR, MTW, and TON. To span a large set of initial conditions, poses were created using different OSDA loadings and conformations, and zeolite supercells. In total, 3,366 poses were generated, optimized using force field calculations, and assigned

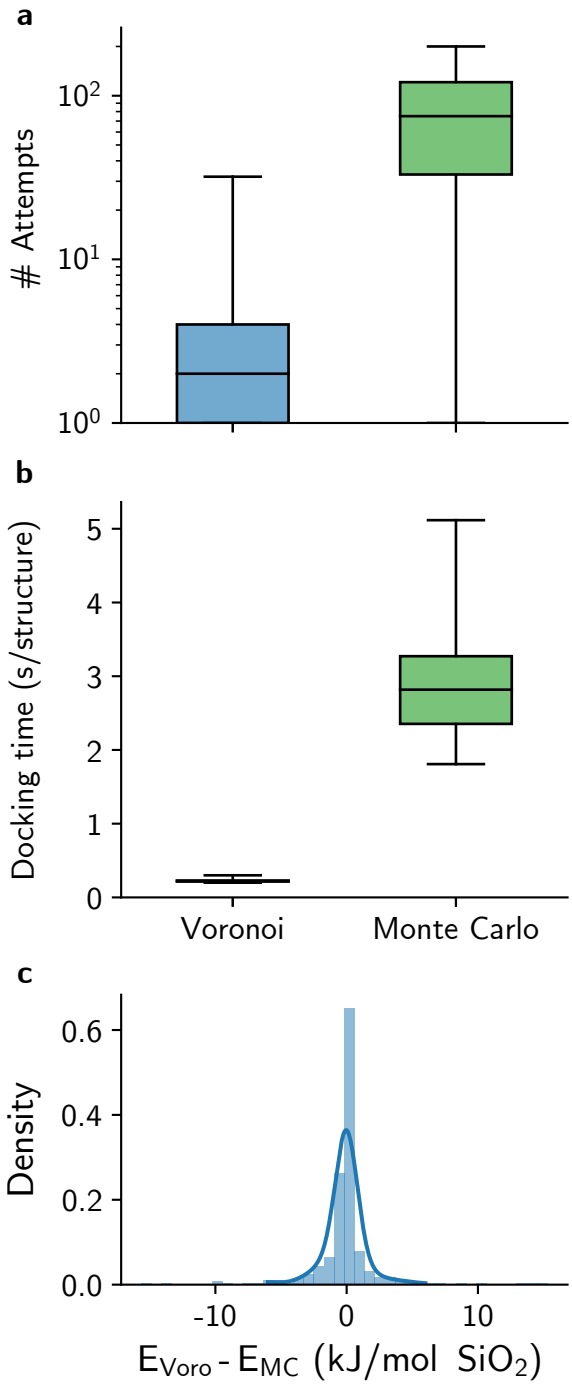

Figure 3: Distribution of **a**, number of attempts, and **b**, docking time per generated structure for Voronoi and Monte Carlo algorithms, as tested by 1,000 independent runs of docking TMAda+ into CHA. The horizontal line is the median, boxes are the interquartile region, and whiskers span the range of the distribution. **c**, Differences of energies between complexes docked with Voronoi (E_{Voro}) and Monte Carlo (E_{MC}) methods. The difference is computed from the minimum of energy found for each optimized pose given a complex and a loading.

a corresponding binding energy. The Monte Carlo algorithm was successful in generating a stable structure for 113 different complexes, whereas the Voronoi docking scheme generated stable structures for 107 of them. We found that binding energies resulting from Voronoi-docked poses are, on average, 0.12 kJ/mol SiO_2 lower than those generated by the Monte Carlo algorithm. Fig. 3c shows the distribution of energy differences when poses of the same complex with equal loadings are compared.

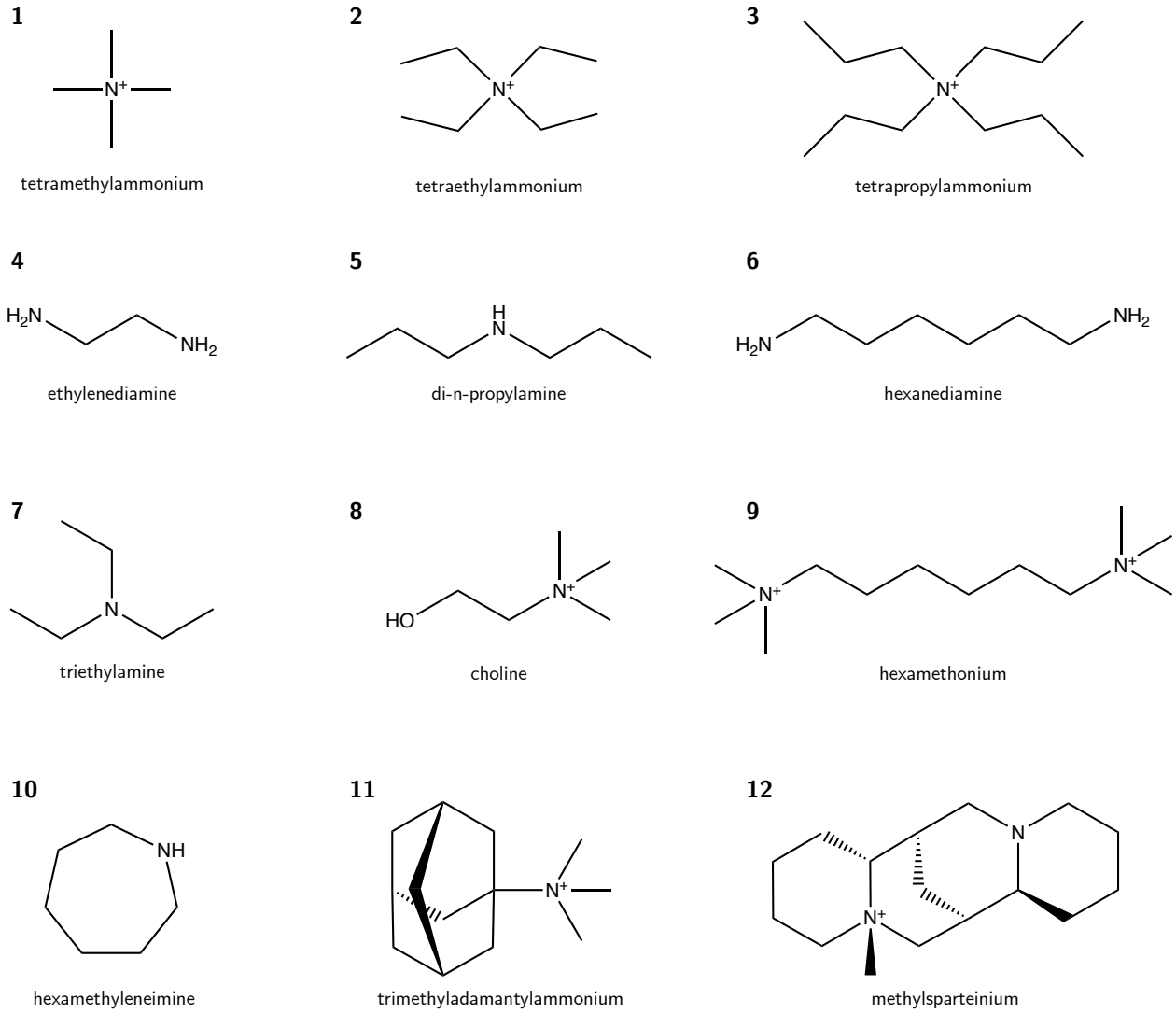

Figure 4: Molecules under study and their names. These OSDAs are typically used in the literature for the synthesis of various zeolites and cover different sizes, shapes and flexibility.

Fig. 5a shows the final binding energies for each complex (see Fig. S5 for the numerical values of energies). The FER-tetrapropylammonium and TON-tetrapropylammonium

pairs, for which no docking attempt was successful, are shown in gray. To assess the ability of VOID to consistently find low-energy poses for frameworks and molecules, rankings of each OSDA against its peers along a given framework are shown in Fig. 5b. Several classical cases of OSDA-zeolite complexes from the literature rank among the strongest-binding per framework, thus validating the ability of our software to find relevant low-energy poses that correlate with experiment. This includes the following pairs: tetramethylammonium with LTA;[41,42] tetraethylammonium with AFI,[43] CHA,[44] and MOR;[45] tetrapropylammonium with AFI,[46] and MFI;[47] di-n-propylamine with AEL;[46] 1,6-hexanediamine with MFI,[48] and TON;[49] hexamethyleneimine with FER;[50] TMAda+ with AFI,[51] and CHA;[44] and methylsparteinium with AFI.[52,53] The analysis also highlights other OSDA-zeolite pairs with favorable binding energies that have not been reported in the literature, to the extent of our knowledge. Some examples of pairs still unrealized are: di-n-propylamine and 1,6-hexanediamine with FER and MOR; triethylamine with AEL and MTW; and hexamethyleneimine with *BEA, LTA, and MTW.

Despite the success of this classification in explaining experimental outcomes of zeolite synthesis, it is unable to recover some instances of OSDA-zeolite pairs from the literature. Some examples of low-ranked OSDAs with strong evidence of structure-direction capacity include: tetraethylammonium with *BEA,[54] and MTW;[55] triethylamine with AFI;[43] and choline with CHA.[56] Nevertheless, most of these molecules display favorable binding energies towards the zeolites of interest. For instance, tetraethylammonium has a binding energy of -10.2 kJ/mol SiO_2 towards *BEA, and choline has a binding energy towards CHA equal to -11.0 kJ/mol SiO_2. Similar binding energies for experimentally-realized OSDA-zeolite pairs have been reported in previous studies.[7,16] Other sources of error in energy calculations may also influence the results. The predictive power of the method is limited mostly by the accuracy of the force field in modeling van der Waals interactions and by the disregard for framework composition when calculating binding energies. From the experimental perspective, other synthesis conditions, such as presence of seeds or defects, temperature, or gel

composition may play an important role in structure direction and compensate for an OSDA with slightly smaller binding energy.

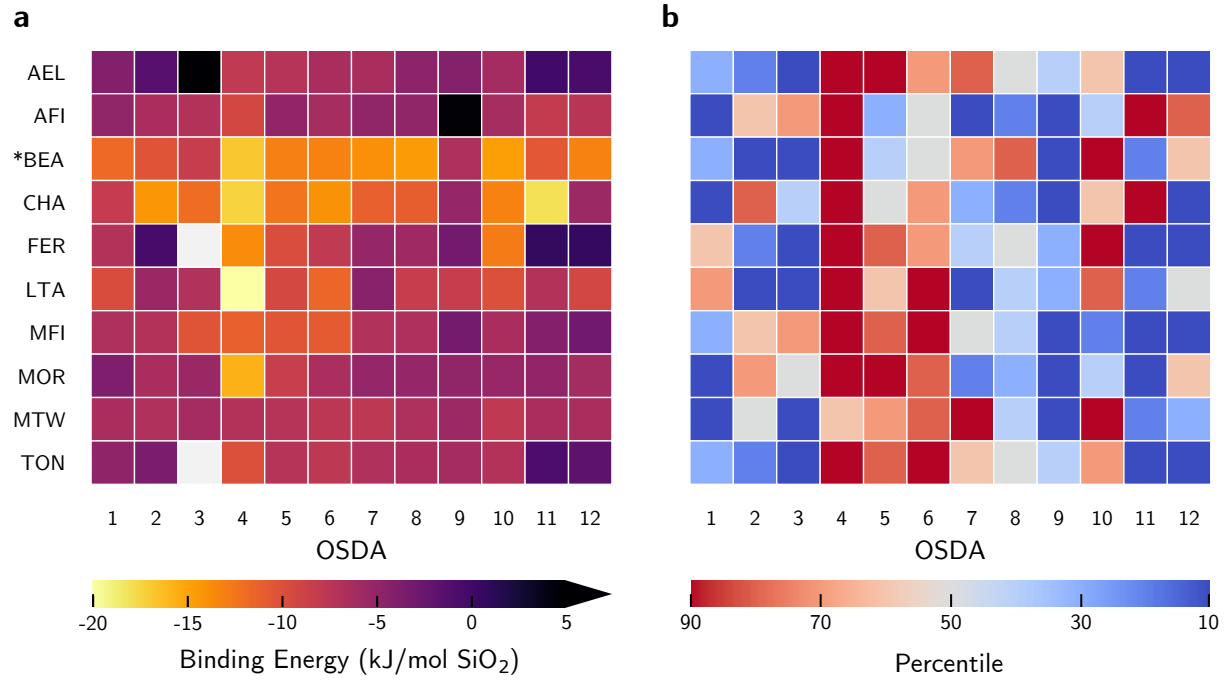

Figure 5: **a**, Binding energies and **b**, their percentiles for the most stable zeolite-OSDA poses from Voronoi and Monte Carlo docking. Lower binding energies are better in terms of stabilization. OSDAs are labeled according to Fig. 4.

Finally, VOID can be applied not only to zeolites, but to other materials as well. Fig. S6 shows two distinct applications of the software to a metal-organic framework (MOF) and a Ni(111) surface. The Voronoi docking method can be used to automate the generation of conformations of molecules inside the MOF, as well as place adsorbates over surfaces according to a distance threshold (e.g. the fitness function in Eq. (4)). The generality and speed of the method and software will prove useful for high-throughput calculations in the field of porous materials and beyond.

Conclusion

In this paper, we have introduced a Voronoi docking algorithm for generating poses of molecules in porous materials, and VOID, an open-source Python package implementing

different docking methods. We showed that Voronoi docking can generate poses of OSDAs in zeolites up to 95 times faster than traditional Monte Carlo methods. We then applied the software to study 120 zeolite-OSDA pairs of high commercial interest. Atomistic simulations demonstrate that host-guest interactions from VOID-generated poses explain outcomes for several synthesis outcomes from the literature. This validates the computational approach and provides novel suggestions of OSDAs to synthesize known zeolite structures. VOID is a general-purpose tool for docking molecules in materials and will prove useful for high-throughput computational screening of complex interfaces.

Acknowledgement

This work was supported by the MIT Energy Initiative (MITEI) and MIT International Science and Technology Initiatives (MISTI) Seed Funds. D.S.-K. was additionally funded by the MIT Energy Fellowship. We thank E. Olivetti, M. Moliner, Y. Román-Leshkov, Z. Jensen, S. Kwon, and S. Bagi for the discussions. Computer calculations were executed at the Massachusetts Green High-Performance Computing Center with support from MIT Research Computing.

Supporting Information Available

Figures S1-S6.

References

(1) Davis, M. E. Ordered porous materials for emerging applications. *Nature* **2002**, *417*, 813–821.

(2) Baerlocher, C.; McCusker, L. B.; Olson, D. H. *Atlas of Zeolite Framework Types*, 6th ed.; Elsevier Science: Amsterdam, 2007; p 404.

(3) Ch. Baerlocher and L.B. McCusker, Database of Zeolite Structures. *http://www.iza-structure.org/databases/* **2020**,

(4) Lobo, R. F.; Zones, S. I.; Davis, M. E. Structure-direction in zeolite synthesis. *Journal of Inclusion Phenomena and Molecular Recognition in Chemistry* **1995**, *21*, 47–78.

(5) Cundy, C. S.; Cox, P. A. The hydrothermal synthesis of zeolites: History and development from the earliest days to the present time. *Chemical Reviews* **2003**, *103*, 663–701.

(6) Cundy, C. S.; Cox, P. A. The hydrothermal synthesis of zeolites: Precursors, intermediates and reaction mechanism. *Microporous and Mesoporous Materials* **2005**, *82*, 1–78.

(7) Burton, A. W.; Zones, S. I.; Elomari, S. The chemistry of phase selectivity in the synthesis of high-silica zeolites. *Current Opinion in Colloid and Interface Science* **2005**, *10*, 211–219.

(8) Moliner, M.; Rey, F.; Corma, A. Towards the Rational Design of Efficient Organic Structure-Directing Agents for Zeolite Synthesis. *Angewandte Chemie International Edition* **2013**, *52*, 13880–13889.

(9) Gallego, E. M.; Portilla, M. T.; Paris, C.; León-Escamilla, A.; Boronat, M.; Moliner, M.; Corma, A. "Ab initio" synthesis of zeolites for preestablished catalytic reactions. *Science* **2017**, *355*, 1051–1054.

(10) Schwalbe-Koda, D.; Jensen, Z.; Olivetti, E.; Gómez-Bombarelli, R. Graph similarity drives zeolite diffusionless transformations and intergrowth. *Nature Materials* **2019**, *18*, 1177–1181.

(11) Gies, H.; Marker, B. The structure-controlling role of organic templates for the synthesis of porosils in the systems SiO2/template/H2O. *Zeolites* **1992**, *12*, 42–49.

(12) Lewis, D. W.; Freeman, C. M.; Catlow, C. R. Predicting the templating ability of organic additives for the synthesis of microporous materials. *Journal of Physical Chemistry* **1995**, *99*, 11194–11202.

(13) Catlow, C. R. A.; Coombes, D. S.; Lewis, D. W.; Pereira, J. C. G. Computer Modeling of Nucleation, Growth, and Templating in Hydrothermal Synthesis. *Chemistry of Materials* **1998**, *10*, 3249–3265.

(14) Nakagawa, Y.; Lee, G. S.; Harris, T. V.; Yuen, L. T.; Zones, S. I. Guest/host relationships in zeolite synthesis: Ring-substituted piperidines and the remarkable adamantane mimicry by 1-azonio spiro [5.5] undecanes. *Microporous and Mesoporous Materials* **1998**, *22*, 69–85.

(15) Wagner, P.; Nakagawa, Y.; Lee, G. S.; Davis, M. E.; Elomari, S.; Medrud, R. C.; Zones, S. I. Guest/host relationships in the synthesis of the novel cage-based zeolites SSZ-35, SSZ-36, and SSZ-39. *Journal of the American Chemical Society* **2000**, *122*, 263–273.

(16) Burton, A. W.; Lee, G. S.; Zones, S. I. Phase selectivity in the syntheses of cage-based zeolite structures: An investigation of thermodynamic interactions between zeolite hosts and structure directing agents by molecular modeling. *Microporous and Mesoporous Materials* **2006**, *90*, 129–144.

(17) Simancas, R.; Dari, D.; Velamazán, N.; Navarro, M. T.; Cantín, A.; Jordá, J. L.; Sastre, G.; Corma, A.; Rey, F. Modular organic structure-directing agents for the synthesis of zeolites. *Science* **2010**, *330*, 1219–1222.

(18) Li, J.; Corma, A.; Yu, J. Synthesis of new zeolite structures. *Chemical Society Reviews* **2015**, *44*, 7112–7127.

(19) Davis, T. M.; Liu, A. T.; Lew, C. M.; Xie, D.; Benin, A. I.; Elomari, S.; Zones, S. I.;

Deem, M. W. Computationally Guided Synthesis of SSZ-52: A Zeolite for Engine Exhaust Clean-up. *Chemistry of Materials* **2016**, *28*, 708–711.

(20) Brand, S. K.; Schmidt, J. E.; Deem, M. W.; Daeyaert, F.; Ma, Y.; Terasaki, O.; Orazov, M.; Davis, M. E. Enantiomerically enriched, polycrystalline molecular sieves. *Proceedings of the National Academy of Sciences of the United States of America* **2017**, *114*, 5101–5106.

(21) Kumar, M.; Berkson, Z. J.; Clark, R. J.; Shen, Y.; Prisco, N. A.; Zheng, Q.; Zeng, Z.; Zheng, H.; McCusker, L. B.; Palmer, J. C.; Chmelka, B. F.; Rimer, J. D. Crystallization of Mordenite Platelets using Cooperative Organic Structure-Directing Agents. *Journal of the American Chemical Society* **2019**, *141*, 20155–20165.

(22) Freeman, C. M.; Catlow, C. R. A.; Thomas, J. M.; Brode, S. Computing the location and energetics of organic molecules in microporous adsorbents and catalysts: a hybrid approach applied to isometric butenes in a model zeolite. *Chemical Physics Letters* **1991**, *186*, 137–142.

(23) Gálvez-Llompart, M.; Cantín, A.; Rey, F.; Sastre, G. Computational screening of structure directing agents for the synthesis of zeolites. A simplified model. *Zeitschrift fur Kristallographie - Crystalline Materials* **2019**, *234*, 451–460.

(24) Pophale, R.; Daeyaert, F.; Deem, M. W. Computational prediction of chemically synthesizable organic structure directing agents for zeolites. *Journal of Materials Chemistry A* **2013**, *1*, 6750–6760.

(25) Daeyaert, F.; Deem, M. W. Design of Organic Structure-Directing Agents for the Controlled Synthesis of Zeolites for Use in Carbon Dioxide/Methane Membrane Separations. *ChemPlusChem* **2019**, *84*, 1–9.

(26) Muraoka, K.; Chaikittisilp, W.; Okubo, T. Multi-objective de novo molecular design

of organic structure-directing agents for zeolites using nature-inspired ant colony optimization. *Chemical Science* **2020**, *11*, 8214–8223.

(27) Lewis, D. W.; Willock, D. J.; Catlow, C. R. A.; Thomas, J. M.; Hutchings, G. J. De novo design of structure-directing agents for the synthesis of microporous solids. *Nature* **1996**, *382*, 604–606.

(28) Willock, D. J.; Lewis, D. W.; Catlow, C. A.; Hutchings, G. J.; Thomas, J. M. Designing templates for the synthesis of microporous solids using de novo molecular design methods. *Journal of Molecular Catalysis A: Chemical* **1997**, *119*, 415–424.

(29) Willems, T. F.; Rycroft, C. H.; Kazi, M.; Meza, J. C.; Haranczyk, M. Algorithms and tools for high-throughput geometry-based analysis of crystalline porous materials. *Microporous and Mesoporous Materials* **2012**, *149*, 134–141.

(30) Pinheiro, M.; Martin, R. L.; Rycroft, C. H.; Jones, A.; Iglesia, E.; Haranczyk, M. Characterization and comparison of pore landscapes in crystalline porous materials. *Journal of Molecular Graphics & Modelling* **2013**, *44*, 208–219.

(31) Ong, S. P.; Richards, W. D.; Jain, A.; Hautier, G.; Kocher, M.; Cholia, S.; Gunter, D.; Chevrier, V. L.; Persson, K. A.; Ceder, G. Python Materials Genomics (pymatgen): A robust, open-source python library for materials analysis. *Computational Materials Science* **2013**, *68*, 314–319.

(32) Sliwoski, G.; Kothiwale, S.; Meiler, J.; Lowe, E. W. Computational methods in drug discovery. *Pharmacological Reviews* **2014**, *66*, 334–395.

(33) Metropolis, N.; Ulam, S. The Monte Carlo Method. *Journal of the American Statistical Association* **1949**, *44*, 335.

(34) Gale, J. D. GULP: A computer program for the symmetry-adapted simulation of solids. *Journal of the Chemical Society-Faraday Transactions* **1997**, *93*, 629–637.

(35) Gale, J. D.; Rohl, A. L. The General Utility Lattice Program (GULP). *Molecular Simulation* **2003**, *29*, 291–341.

(36) Mayo, S. L.; Olafson, B. D.; Goddard, W. A. DREIDING: A generic force field for molecular simulations. *Journal of Physical Chemistry* **1990**, *94*, 8897–8909.

(37) Sanders, M. J.; Leslie, M.; Catlow, C. R. Interatomic potentials for SiO2. *Journal of the Chemical Society, Chemical Communications* **1984**, 1271–1273.

(38) Landrum, G. RDKit: Open-source cheminformatics. 2006; `www.rdkit.org`.

(39) Halgren, T. A. Merck molecular force field. I. Basis, form, scope, parameterization, and performance of MMFF94. *Journal of Computational Chemistry* **1996**, *17*, 490–519.

(40) Tosco, P.; Stiefl, N.; Landrum, G. Bringing the MMFF force field to the RDKit: implementation and validation. *Journal of Cheminformatics* **2014**, *6*.

(41) Barrer, R. M.; Denny, P. J. 202. Hydrothermal chemistry of the silicates. Part X. A partial study of the field CaO-Al2O3-SiO2-H2O. *Journal of the Chemical Society (Resumed)* **1961**, *60*, 983–1000.

(42) Kerr, G. T. Chemistry of Crystalline Aluminosilicates. II. The Synthesis and Properties of Zeolite ZK-4. *Inorganic Chemistry* **1966**, *5*, 1537–1539.

(43) Flanigen, E. M.; Lok, B. M.; Wilson, S. T. Crystalline metallophosphate compositions. *US Patent 4,310,440* **1982**,

(44) Zones, S. Zeolite SSZ-13 and its method of preparation. *US Patent 4,544,538* **1985**,

(45) Jacobs, P. A.; Martens, J. A. *Studies in Surface Science and Catalysis*; Elsevier Inc., 1987; Vol. 33; pp 321–348.

(46) Flanigen, E. M.; Lok, B. M.; Patton, R. L.; Wilson, S. T. Aluminophosphate molecular sieves and the periodic table. *Pure and Applied Chemistry* **1986**, *58*, 1351–1358.

(47) Argauer, R. J.; Landolt, G. R. Crystalline zeolite ZSM-5 and method for preparing the same. *US Patent 3,702,886* **1969**,

(48) Rollmann, L. D.; Valyocsik, E. W. Synthesis of zeolite ZSM-5. *US Patent 4,139,600* **1979**,

(49) Araya, A.; Lowe, B. M. Synthesis and characterization of zeolite Nu-10. *Zeolites* **1984**, *4*, 280–286.

(50) Rubin, M. K. Synthesis of crystalline ZSM-35 structure. *US Patent 4,925,548* **1990**,

(51) Zones, S. I.; Van Nordstrand, R. A.; Santilli, D. S.; Wilson, D. M.; Yuen, L.; Scampavia, L. D. Sequence of High Silica Zeolites Found During Synthesis Experiments in The Presence of A Quaternary Adamantammonium Cation. *Studies in Surface Science and Catalysis* **1989**, *49*, 299–309.

(52) Nakagawa, Y. Process for preparing molecular sieves using a sparteine template. *US Patent 5,271,992* **1993**,

(53) Lobo, R. F.; Davis, M. E. Synthesis and characterization of pure-silica and boron-substituted SSZ-24 using N(16) methylsparteinium bromide as structure-directing agent. *Microporous Materials* **1994**, *3*, 61–69.

(54) Kerr, G. T.; Rosinski, E. J.; Wadlinger, R. L.; Kerr, G. T.; Rosinski, E. J. Catalytic composition of a crystalline zeolite. *US Patent 3,308,069* **1964**,

(55) Rosinski, E.; Rubin, M. Crystalline Zeolite ZSM-12. *US Patent 3,832,449* **1974**,

(56) Xu, R.; Zhang, R.; Liu, N.; Chen, B.; Zhang Qiao, S. Template Design and Economical Strategy for the Synthesis of SSZ-13 (CHA-Type) Zeolite as an Excellent Catalyst for the Selective Catalytic Reduction of NOx by Ammonia. *ChemCatChem* **2015**, *7*, 3842–3847.

Graphical TOC Entry

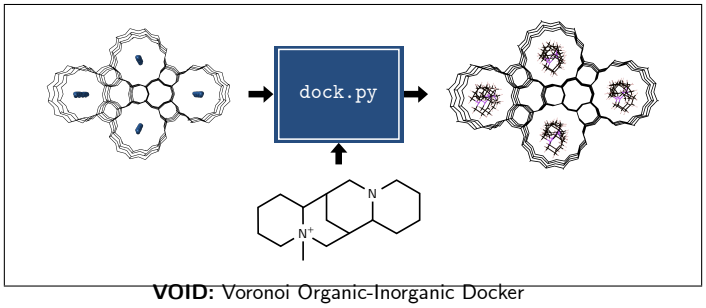

VOID: Voronoi Organic-Inorganic Docker